CIWC 2019

sciforum

Conference Proceedings Paper

Enhancement of Tribological Behavior of ZrCN Coating

Isabel Clavería [1,*], Aleida Lostalé [1], Cristina Zubizarreta [2], Gemma Mendoza [2], Ángel Fernández [1], Pere Castell [3], and Daniel Elduque [1]

[1] Mechanical Department, University of Zaragoza EINA, Maria de Luna 3, 50018 Zaragoza, Spain; aleida.lostale@fersa.com (A.L.); afernan@unizar.es (Á.F.); delduque@unizar.es (D.E.)
[2] Fundación Tekniker, Calle Iñaki Goenaga, 5, 20600 Eibar, Spain; cristina.zubizarreta@tekniker.es (C.Z.); gemma.mendoza@tekniker.es (G.M.)
[3] AITIIP Foundation, Calle Romero 12, 50720 Zaragoza, Spain; pere.castell@aitiip.com
* Correspondence: isabel.claveria@unizar.es; Tel.: +34-876-555-234

Received: 15 February 2019; Accepted: 7 March 2019; Published: 8 March 2019

Abstract: This paper focuses on tribological behavior of ZrCN coating on bearing steel substrates DIN 17230, 100Cr6/1.3505, fulfilling also roughness and adherence requirements. Two strategies are followed to achieve a reduction of coefficient of friction. Initially, a low roughness coating by using physical vapor deposition (PVD sputtering process) is developed. At this stage, PVD conditions guarantying adherence and avoiding drops generated during that process are achieved. A second strategy consisting of application of several polish post-processes is proposed. These polish post-processes pretend to reduce roughness keeping, at the same time, a proper adherence. Different post-process durations and conditions are analyzed to achieve positive adherence results. Coated bearing samples obtained from the application of these two strategies are tested in friction test rigs. These tests conclude that there is not a significant improvement friction performance by applying ZrCN coatings compared to bearing baseline.

Keywords: PVD; polish; Zr(C,N); coating; bearing; roughness; adherence; friction torque

1. Introduction

Roller bearings are components with numerous uses for rotating applications, particularly in automotive industry. According to recent studies [1], of every liter of fuel used in an average vehicle, 5% is consumed in mechanical losses, and 1% of the total is lost in the simple operation of the bearings. Energy efficiency and the reduction of fuel consumption and polluting emissions are aspects increasingly demanded by users and manufacturers. This trend is noticed with the appearance of more efficient products, which may even be different from the standard versions in terms of dimensions, assembly or new materials.

Despite above mentioned bearing losses, these mechanical components exhibit very low friction in lubricated conditions (friction coefficient < 0.05), provided also by the rectangular shaped "line contact" between the roller and the outer and inner rings [2–5]. The contact pressures may vary from 0.5 up to 3 GPa, depending on the application [2,3]. The rolling operation abides by the elastohydrodynamic (EHD) theory and it is characterized by the thickness of the lubricant film formed during rolling [6–8]. Important factors defining the conditions of rolling operation are the surface roughness of the counterparts and the stress distribution at the subsurface (from 50 to 150 μm underneath the surface) from the contact between the counterparts [9–12]. So, nowadays, it is commonly expected that tribology can contribute to the following technical considerations: improvement of the fuel consumption efficiency through friction reduction, lightweight construction, downsizing through resistance increase to higher Hertzian contact pressures, waste reduction thanks to lower wear and less frequent oil changes as well as and use of more environment friendly lubricants (Bio-no-tox).

There are different methods for reducing friction on bearings. These methods go from updating internal bearing geometry to changing bearing component materials (e.g., plastic cages made of nano-additivated plastics to achieve self-lubricant behavior) [13], new lubricants development or coating rolling bearing surface.

Thin coatings are nowadays an interesting and low-cost approach for solving technical problems since their properties can be infinitely varied and combined without implying a complete change of the original conception of mechanical components. Deposition of a protective low friction coating on the surface of the rollers extends the lifetime of the component [2,14–16]. In many cases, where a coating is deposited on a steel component, lifetime of the component is increased and its tribological response improved [17–21]. The overall performance of the coated surfaces is also determined by the coating/substrate interface tolerance to crack propagation [14,17]. It has been demonstrated that coatings produced by physical vapor deposition (PVD) may withstand higher shear stress levels during rolling than coatings produced by chemical vapor deposition (CVD) or thermal spray [16,22]. TiN, TiAlN, TiC, CrN, Cu, and diamond-like carbon (DLC) coatings, produced by PVD, have already been studied in rolling-contact fatigue (RCF) tests improving the lifetime of the components [17–19,23–25]. DLC and carbon nitride (CN) coatings are considered good candidates for use in rolling components as they provide low friction and high wear resistance [26,27].

In this study, Zr(C,N) and also ZrC thin coatings are considered because they are successfully tested at a lubricant temperature of 120 °C and thus until average Hertzian pressures of 1.94 GPa [28]. From these results, this composition arises as a promising coating to be used in bearings for automotive industry (differential applications) because they stand similar working temperatures and contact stresses. Hardly any previous study has been carried out with the combination Zr(C,N)coating on bearings. In Reference [15] this kind of coating is used for rolling bearings, but results measured are more focused on properties of the bearing material than on functional results as friction torque as it is revealed in this paper.

2. Materials and Methods

2.1. .Materials

2.1.1. Substrate

Bearing steel 100Cr6 (according to ISO 683-17 [29]) has been used as PVD substrate. In this study, a through hardening bearing steel with the following chemical composition is used: carbon (0.93%–1.05%), manganese (0.25%–1.20%), chromium (0.90%–1.60%), molybdenum (0%–0.10%), and nickel (0%–0.25%). Other residual that can also be found are: oxygen (max. 10–15 ppm), aluminum (max. 0.050%), titanium (max. 30–50 ppm), and calcium (max. 10 ppm) [30].

Due to endurance strength, distribution must compensate equivalent stress level and, therefore, steel has to be subjected to a martensitic through hardening treatment adjusting surface hardness to 59–63 HRC at a temperature of 180–200 °C. These HRC values are minimum for a dynamic capacity of 100%.

2.1.2. Bearing Samples

Tapered roller bearing (TRB) 594A/592A belonging to TRB inches family from FERSA BEARINGS SA (Zaragoza, Spain) and used for differential application in heavy duty vehicles is chosen as sample to be coated. Shape and dimensions are shown in Figure 1. Coated surfaces are contact surfaces between Components 2 and 3 in Figure 1.

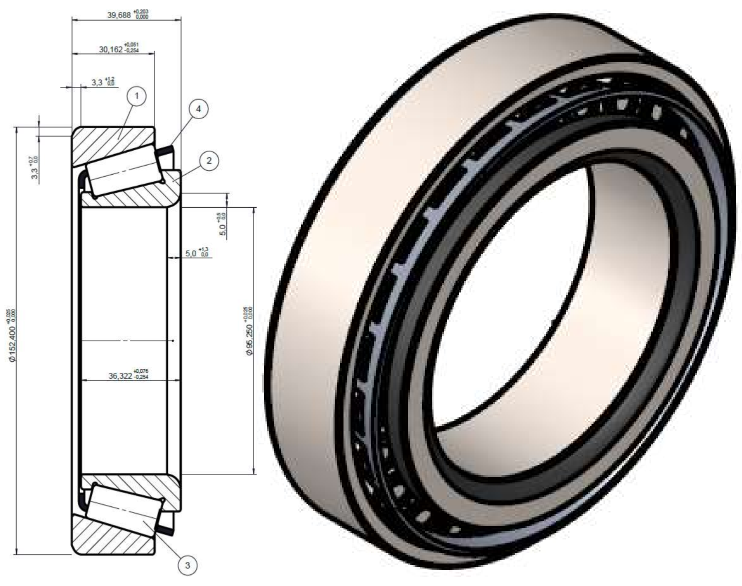

Figure 1. Tapered roller bearing 594A/592A.

2.1.3. Coating Layer

Materials used for coating layer creation are Zr target from Robeko (Šibenik, Croatia), purity R60702, ≥99.5 wt % and Ti target from Robeko, purity grade 2, 99.5% weight. Hydrogen in Argon (20%); Alphagaz 2 Argon (purity ≥ 99.9999 mol %); Alphagaz 2 Nitrogen (purity ≥ 99.9999 mol %) and Alphagaz 1 Acetylene (purity ≥ 99.6 mol %) from Air Liquide (Paris, France) are used as reactive gases.

2.2. Equipment and Experimental

2.2.1. PVD Coating Process

Prior to PVD deposition, sample substrates are cleaned under a degreasing-solvent sequence. Once loaded in the vacuum chamber, it is evacuated up to a pressure of 10−4 mbar. Then Glow Discharge cleanliness stage consisting on applying a voltage under vacuum conditions on the samples in an atmosphere of argon mixed with hydrogen is applied to bearing samples. A high negative bias of −600V is applied on the samples at the beginning of the deposition step, and then decreased progressively during the first steps of the deposition sequence to −30 V.

ZrCN coatings are deposited by physical vapor deposition (PVD) technique using cathodic arc evaporation (CAE) method to deposit titanium-zirconium-based coatings on rolling bearing surface. CAE method consists of applying a voltage of several hundred volts between an anode and the positively charged arc cathode in presence of argon gas in a vacuum chamber melting or evaporating tiny quantities of material. Approximately 90% of the evaporated cathode particles form positively charged metal ions. A bias voltage is now applied between the vacuum chamber and the substrate. This accelerates the metal ions in the direction of the sample surface. A reaction between metal ions and a reactive gas (nitrogen and hydrocarbon) fed in externally is produced leading to deposition of the ions on the sample as a fine carbonitride layer.

The process is carried out with an industrial equipment MIDAS 775 designed and manufactured by Tekniker [31] with the following features: vacuum chamber volume Ø750 mm × 750 mm; 12 circular arc evaporators (Ø100 mm) in four columns; 45 kW pulsed DC bias power supply system up to 1000 V consisting of two MDX II DC and one SPARC-VS pulsing unit from Advanced Energy (Fort Collins, CO, USA); working intensity range of 60–200 A; maximum temperature substrates of 500 °C, and N_2, C_2H_2, O_2 reactive gases.

Four different PVD coatings designs have been developed by using 4 metallic evaporators (2Ti, 2Zr), and introducing Nitrogen gas (N_2) and acetylene (C_2H_2) in reactive process as described in Table 1. Arc intensity of Titanium and Zirconium targets is set at 120 and 140 A respectively. Each coating design consists of different layers to provide the tribological properties required to reduce friction during bearing performance. In order to improve the coating adhesion a pure titanium interlayer is deposited in all the coating designs using a high bias voltage of 400–30 V. Then, a second Ti–Zr interlayer is applied in designs D1, D2 and D4. In case of D3 a second interlayer of TiN instead of TiZr is deposited, as well as a third interlayer of Ti–Zr–N. For D4 design an additional bilayer of ZrN is formed.

Table 1. Composition of PVD coating designs.

Coating Design	Layer Composition	Deposition (min)				Layer Configuration	Resistance Temperature (°C)
		Ti	Ti–Zr	TiN	Ti–Zr–N		
D1	Ti + Ti–Zr	60	5	0	0	ZrCN multilayer	250
D2	Ti + Ti–Zr	5	1	0	0	ZrCN multilayer	250
D3	Ti + TiN + Ti–Zr–N	1	0	4	1	ZrCN multilayer	250
D4	Ti + Ti–Zr	60	5	0	0	ZrCN multilayer + ZrN bilayer	250

2.2.2. Post-Polish Process

A polishing post-process is carried out after PVD deposition on bearings samples following two different methods. Method A uses walnut shell as abrasive in an OTEC DF 35 machine (OTEC Präzisionsfinish GmbH, Straubenhardt-Conweiler, Germany), which is a spindle abrasive finishing machine, with 3 workplace holders, .75 kW, 230 volt motor with octagonal stainless steel process container and controls. Method B uses walnut shell additivated with a silica base abrasive (80%) in a Pardus Drag Finish Unit from PD2i machine (Paris, France). In both equipments, samples are introduced in a vessel full of abrasive material in order to polish pieces surface. Method A is defined by applying 30 min steps (15 min each way) at 20 rpm, and Method B is characterized by applying 15 min (1.5 min each way) at 35 rpm. Three configurations have been carried out in order to achieve the best balance between roughness and adherence according to Table 2. In order to prevent peeling-off of coating layer during the process, coating designs D1 and D4 have been considered for post-polishing because they are the ones with higher coating thickness needing to improve roughness, according to first results obtained from PVD tests.

Table 2. Post-polishing process configuration parameters.

Configuration	Method	Time (min)	Rotate Speed (rpm)
A1	A	180	20
A2	A	360	20
B	B	15	35

2.2.3. Geometric Analysis

Before testing coating quality parameters, a complete metrological analysis including shapes, profiles and roundness of bearing raceway and flange is done. Profile characterization is carried out by using a Form Talysurf 120 (Taylor Hobson Ibérica, Barcelona, Spain). This analysis is crucial to know if coated bearing samples to be tested are comparable to baseline design bearing according to allowed limits and shapes agreed by FERSA BEARINGS SA (Zaragoza, Spain). Figure 2 shows inner ring raceway profile (a) and flange profile (b) where geometric analysis is performed.

A second test testing roundness of raceway is performed according to ISO 26423:2009 [32] with a Talyrond 365 with software Ultra by Taylor Hobson V5.21.9.36 both from TAYLOR HOBSON

(Taylor Hobson Ibérica, Barcelona, Spain). Roundness is defined as the separation of two concentric circles that just enclose the circular section of interest, the circular raceway section in this study. Accurate roundness measurement is vital to ensure correct function of bearings avoiding noise and premature failure.

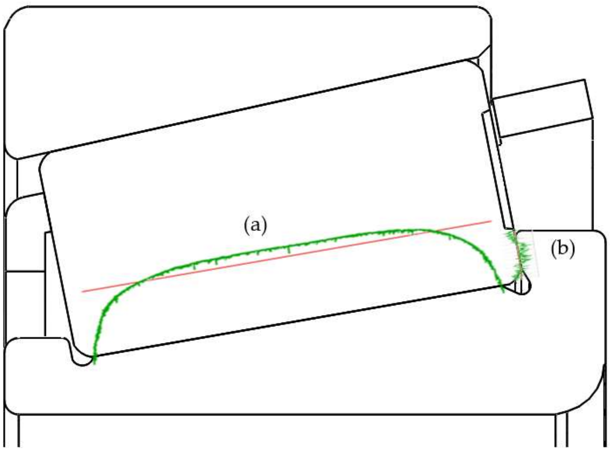

Figure 2. Measured profiles: (**a**) inner ring raceway profile; (**b**) flange profile.

2.2.4. Coating Properties

Coating properties measured to ensure its validity are: roughness (R_a), thickness, hardness, adherence and bearing friction torque.

- Roughness

Perthometer M2 from Mahr (Barcelona, Spain), with a maximum range of 150 µm and a maximum cut-off length of 17.5 mm, is used for measuring roughness of coated samples as Ra (arithmetical mean deviation of the assessed profile) used in standards as DIN EN ISO 4287:1998 [33], ISO 4287:1997 [34] or JIS B 0601:1994 [35]. This equipment uses a mapping method for 2D surface analysis in which a surface is horizontally crossed at constant speed. Mapping profile is superficial profile drawn by analysis needle. Quantification is made by measuring vertical deviations of a real surface comparing to its ideal shape. Cut-off parameter is a profile filter that sets which wave length refers to roughness and which one to waviness. Cut-off parameters set for the tests according to Ra ranges are shown on Table 3. To ensure a proper bearing performance, arithmetical mean deviation of the assessed profile roughness (R_a) must be lower than 0.15 µm according to FERSA BEARINGS SA know-how.

Table 3. Cut-off selection, λ_c according to ISO 4288:1996 [36].

Profile R_a (µm)	Cut-off, λ_c (mm) × n	R_a Evaluation Length, l_n (mm)
(0.006) < $R_a \leq$ 0.02	0.08 × 5	0.4
(0.02)< $R_a \leq$ 0.1	0.25 × 5	1.25
0.1 < $R_a \leq$ 2	0.8 × 5	4
2 < $R_a \leq$ 10	2.5 × 5	12.5

- Thickness

Coating thickness has been determined by means of a calostest test with a Calotest CSEM equipment (DEPHIS, Étupes, France). A ball is turned over the coating until it arrives to substrate producing a spherical crater. Microscope measuring of this dimple diameter allows for knowing coating thickness [37]. Adequate thickness measurement is ranging between 1 and 10 µm for smaller thickness dimple could be too small leading to inaccurate measurements.

- Adherence

A Rockwell C indentation is performed with a load of 150 kg and then trace edges are analyzed by optical microscope to evaluate adherence. A chart VDI 3198 indentation test (Figure 3) is used to set adherence grade [38]. The chart states that the higher crack and delamination number is the worse adherence is. Values from HF1 to HF4 stands for acceptable adherence values, and HF5 and HF6 values stand for non-acceptable adherence values.

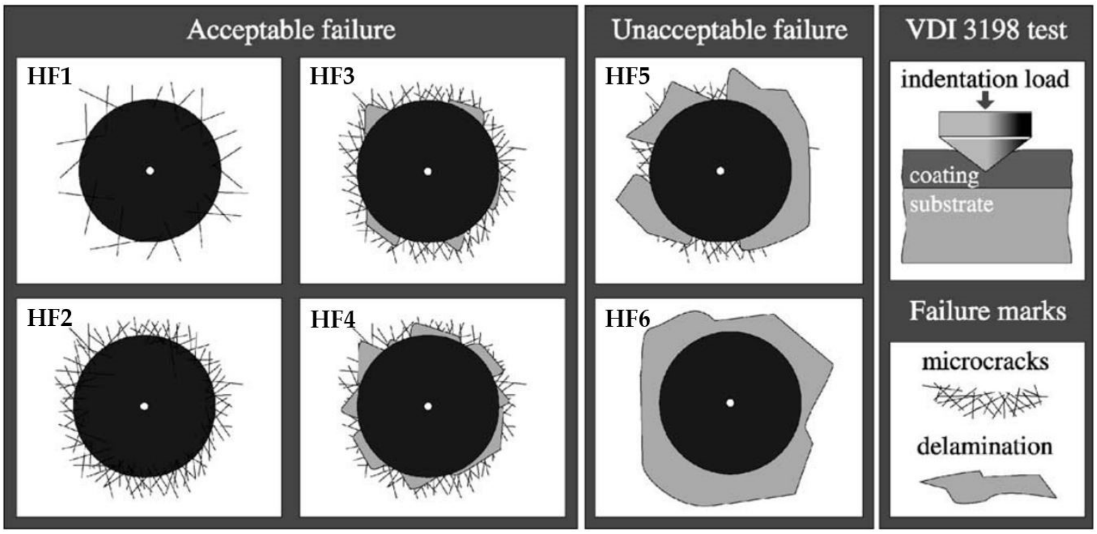

Figure 3. Chart VDI 3198 indentation test.

- Friction torque

Two friction torque test protocols, described on Table 4 are performed to know the behavior of bearings samples under both, low-load and low speed conditions. Stribeck test (ST) determines friction torque at low load and it is useful to determine how the lubrication regime is acting and how much torque bearing is consuming during running-in. Torque to Rotate (TTR) test is used to determine how much torque the bearing consumes under different loads and at low speed. They both offer GO/NO GO threshold to check if the ZrCN coatings peel-off or keep on the bearings during their lifetime. Three coated bearing pairs, named as Set 1, Set 2 and Set 3, plus a pair of uncoated bearings, named as baseline are subjected to the tests. Friction torque tests were carried out in collaboration with FERSA BEARINGS SA in an AX-180 TT test rig where tapered roller bearings were assembled in tandem configuration. Protective oil was applied as bearing lubrication. Test rig characteristics are: test bench size, 450 mm × 1220 mm; No. of stations, 1; No. of bearings, 2; bearing outer diameter size, up to 180 mm; axial load (max.), 15 kN; speed range, 0–1000 rpm; torque (max.), 100 N m.

Table 4. Friction torque test protocols.

Test	Preload (kN)	Speed Range (rpm)	Temperature	Test Time (min)
Stribeck test	8	0–200	room	1.5 min
Torque to Rotate test	0–15 (1.5 kN/step)	30	room	10 min (1 min/load step)

3. Results and Discussion

3.1. Geometrical Analysis

Results of geometrical analysis for raceway profile defined as (a) in Figure 2 are shown in Figure 4. Figure 4a shows raceway profile for uncoated bearing and Figure 4c shows raceway profile for coated bearing. It can be observed that coating has perfectly copied the shape of the raceway logarithmic profile. Figure 4b,d shows a detailed area of the raceway profile (marked as dotted area in Figure 4a,c). It is also confirmed in detailed views that the coating reproduces almost exactly the uncoated railway.

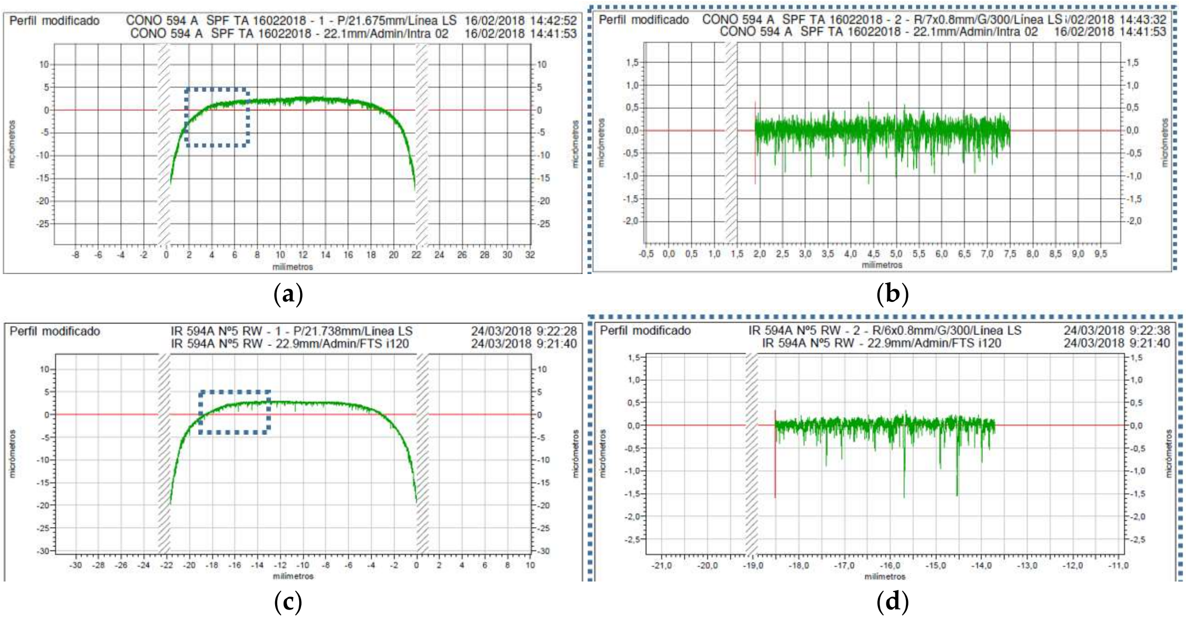

Figure 4. (**a**) Uncoated bearing inner ring raceway profile (logarithmic); (**b**) uncoated bearing inner ring raceway profile at selected area, (**c**) coated bearing inner ring raceway profile (logarithmic); and (**d**) coated bearing inner ring raceway profile at selected area.

Results of geometrical analysis for flange profile which is defined as (b) in Figure 2 are shown in Figure 5. Figure 5a shows the flange profile for uncoated bearing, and Figure 5c shows the flange profile for coated bearing. It can be observed that coating has also perfectly copied the shape of the flange profile. Figure 5b,d shows a detailed area of the flange profile (marked as dotted area in Figure 5a,c). It is also confirmed in detailed views that the coating reproduces almost exactly the uncoated flange.

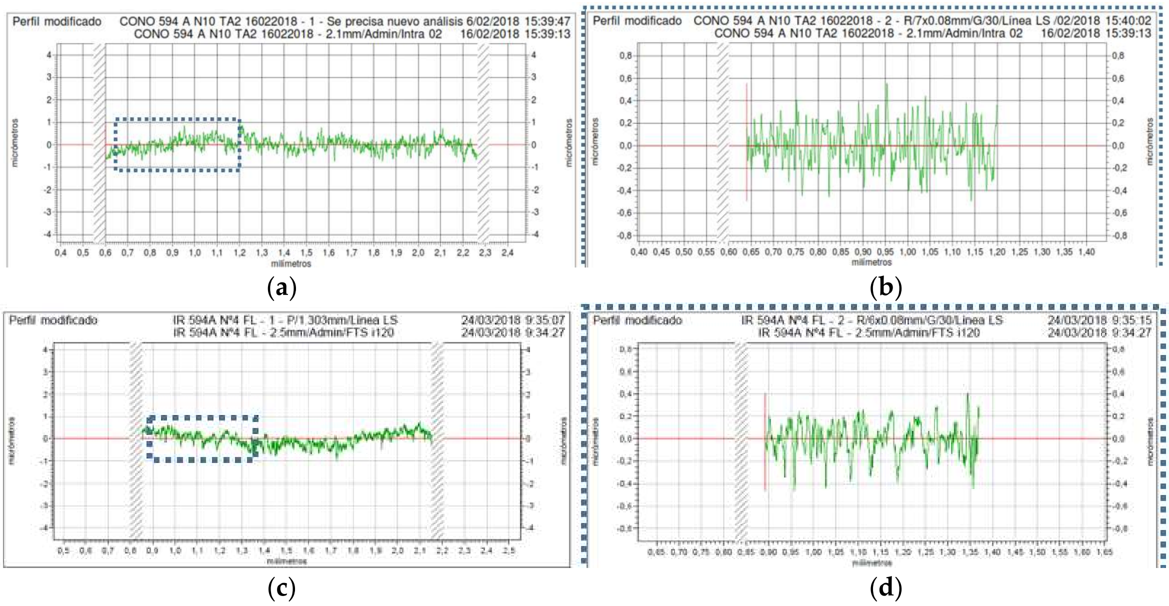

Figure 5. (**a**) Uncoated bearing flange profile (logarithmic); (**b**) uncoated bearing flange profile at selected area, (**c**) coated bearing flange profile (logarithmic); and (**d**) coated bearing flange profile at selected area.

Figure 6 shows RONt distribution at inner ring raceway. RONt values, obtained after PVD coating process, range from 0.82 to 2.34 µm, which are under FERSA BEARINGS SA limit (RONt < 6 µm).

It can be concluded that shapes are good according FERSA BEARINGS SA specification, so coating process has no affection on the profile shapes of the bearing. Thus, it allows to proceed with the roughness, thickness, hardness and adherence tests ensuring that results obtained are comparable to those obtained on the uncoated baseline bearings.

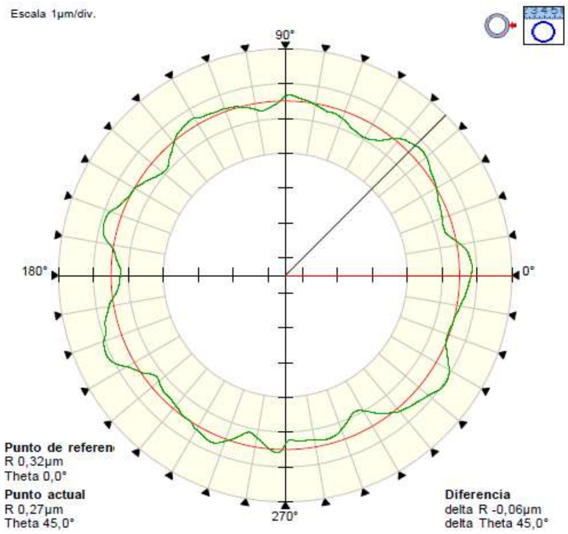

Figure 6. Inner ring raceway diameter shape.

3.2. PVD Coating Results

As described in Table 5, coating design D1 offers a good adherence result HF1 showing neither cracks nor delamination (Figure 7a), but the roughness (R_a) is 0.540, above the allowed value (R_a < 0.15) due to the droplets that can be seen in cross section of the adhesion layer (Ti + Ti–Zr) of D1 coating (Figure 7b,c). These droplets are inherent to the Arc Evaporation coating technology in which a very high grade of ionization can be achieved. But at the same time, these high energies can melt the material to be deposited, with the consequent droplets formation and deposition.

However, for coating design D2, in which times deposition are reduced, bad results in terms of roughness (R_a = 0.240) and adhesion (HF5) (Figure 8a) are achieved, even though roughness value is lower than the one obtained for D1 samples as it can be seen in the reduction of droplet density (Figure 8b). The lack of adhesion is clearly observed in Figure 8a in which grey zones in the trace edge corresponds to the bare substrate, areas where the coating has been removed. Applying a thinner adhesion layer, 5 min of Ti instead of 60, and 1 min of Ti–Zr instead of 5, leads to lower roughness at the expense of substrate-coating adhesion.

Table 5. PVD coating results.

Coating Design	R_a (µm)	Thickness (µm)		Adherence (HF)	Hardness (HRC)	
		Adherence Layer	Total		Before PVD Application	After PVD Application
D1	0.540	1.24	3.67	HF1	60.7	59.0
D2	0.240	0.21	2.61	HF5	60.4	59.1
D3	0.080	0.46	2.86	HF5	60.5	59.7
D4	0.433	1.23	3.74	HF1	59.6	59.2

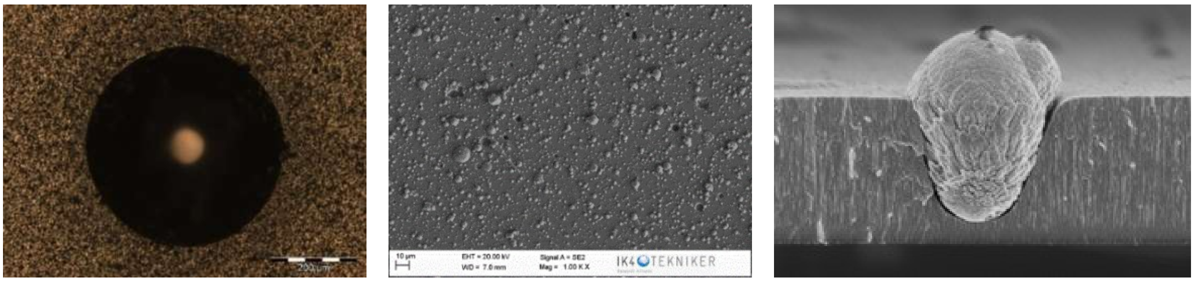

(**a**) (**b**) (**c**)

Figure 7. (**a**) D1 adherence results; (**b**,**c**) D1 adherence layer drops.

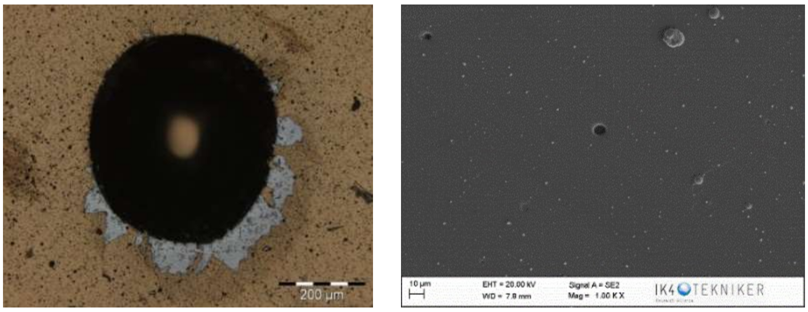

(**a**) (**b**)

Figure 8. (**a**) D2 adherence results; (**b**) D2 adherence layer drops.

D3 coating design includes a new coating composition for adherence layer with a thinner Ti adhesion layer of one minute and then introducing nitrogen at the end trying to improve adhesion through a more progressive transition to the functional multilayer. A proper R_a value of 0.080 is achieved, which can be observed in both surface and cross section micrographs (Figure 9b,c), where a lower density and smaller droplets are observed. But once again, the coating resulted in lack of adhesion HF5 (Figure 9a) as grey areas in the trace edge indicates removal of the coating and the presence of the bare substrate.

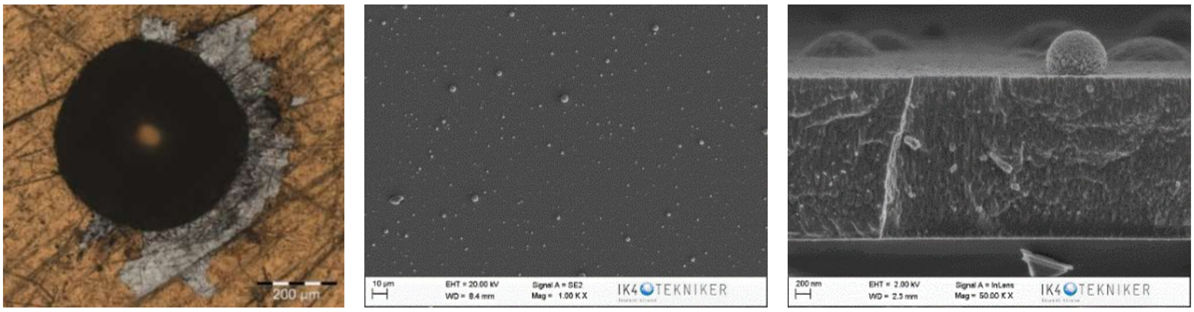

(**a**) (**b**) (**c**)

Figure 9. (**a**) D3 adherence results; (**b**,**c**) D1 adherence layer drops.

For D4 design, a ZrN bilayer is added to D1 design. The new bilayer pretends to increase functional coating thickness for the later post-polishing process, trying to ensure a better roughness keeping adherence performance. Results show that adherence is kept under acceptable values, with a classification of HF1, as can be observed in Figure 10 where any trace of peeling off and bare substrate presence can be observed. In spite of the reduction of roughness value down to 0.433, this value is far from the allowed roughness of 0.15.

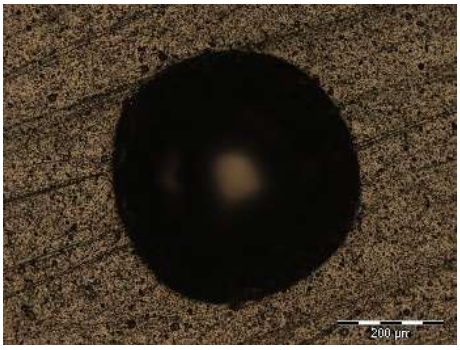

Figure 10. D4 adherence results.

HRC before and after PVD application is shown in Table 5. Samples before PVD application show a HRC value around 60 HRC. After PVD application these values decreases up to values ranging from 59 to 59.7 HRC. Reduction in HRC when applying PVD process is explained by the increasing of temperature on the sample during the cathodic arc application on the bearing steel. This analysis of the samples hardness gives relevant information about the performance of bearing steel after PVD process application. HRC values ranging 59–63 HRC after PVD application indicate that steel of the bearing sample has not reached 180–200 °C, which is tempering temperature of bearing steel, avoiding any deterioration of bearing steel properties. Figure 11a shows that tempering temperature is achieved at 180–200 °C for martensitic bearing steel. Figure 11b gives information about relation between tempering temperature and HRC hardness for martensitic bearing steel. It can be observed that temperature range of 180–200 °C corresponds to a range of 59–63 HRC [39].

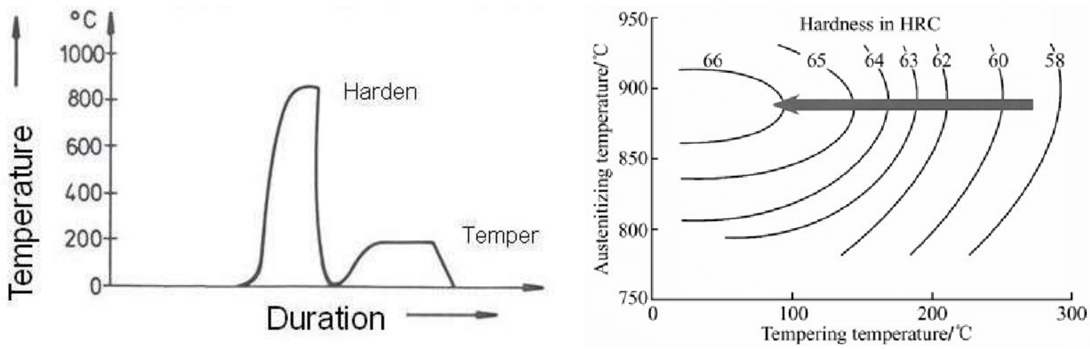

(a) (b)

Figure 11. (**a**) Martensitic through hardening treatment; (**b**) tempering temperature vs. hardness.

Regarding thickness, it can be seen that D1 and D4 coating designs achieve higher values (3.67 and 3.74 µm, respectively) than D2 and D3 coatings designs (2.61 and 2.86 µm, respectively). This is mainly due to the thicker adherence layer obtained for D1 and D4 coatings because PVD process time is longer in D1 and D4 than in D2 and D3. D4 has the thickest coating layer thanks to the addition of a ZrN bilayer.

Due to the fact that is not possible to obtain a compromise between adhesion and low roughness in these PVD processes carried out at low temperature arc evaporation, a post-polish process is proposed to lower roughness. As samples D1 and D4 show acceptable adherence results, but they require roughness improvement, and these samples also present the highest thickness values, they are selected for post-polishing process application in order to improve their roughness. D2 and D3 are discarded due to its low thickness value that could lead to peeling off when applying post-polishing process.

3.3. *Post-Polish Process*

After the analysis of PVD process results, it can be concluded that coating design strategies are not enough to get a proper coating balancing required roughness and adhesion results. For that reason, a post-polish process is applied to lead to a proper combination results. Table 6 shows the results after post-polish process.

Table 6. Post-polish process results.

Coating Design	Post-Polish Configuration	R_a (μm)		Thickness (μm)		Adherence (HRc)
		Before Post-Polish	After Post-Polish	Before Post-Polish	After Post-Polish	
D1	A1	0.540	0.371	3.67	3.30	HF1
	A2	0.540	0.226	3.67	3.25	HF1
	B	0.540	0.171	3.67	2.45	HF1
D4	B	0.433	0.082	3.74	3.45	HF1

After applying post polish Method A during 3 h (polish configuration A1), Samples D1 were measured and then introduced again in vessel to continue post-process up to 6 h (polish configuration A2). R_a values decreases a 31.30% for configuration A1 and a 58.15% for configuration A2. The thickness is reduced 10.08% and 11.44% for configurations A1 and A2 respectively. In case of applying post-polishing method B (configuration B), R_a is reduced by 68.33% up to 0.171 μm and the thickness is lowered up to 2.45 μm. In any case R_a does not achieve FERSA BEARINGS SA allowed value of 0.15. As the most promising results are obtained when applying B configuration, D4 samples are only subjected to this B configuration achieving an acceptable R_a value of 0.082 (reaching a reduction of 81.06%) with a high thickness of 3.45 (only 7.75% reduced from blank sample) and also fulfilling adherence requirements. Figure 12 shows D4 coated samples, postpolished under configuration B and fulfilling roughness and adherence standard.

Figure 12. Bearing samples D4 coating + B polish post-process.

3.3. *Friction Torque*

Samples with D4 coating design and post-polishing configuration B, fulfilling all the functional requirements of R_a, thickness, hardness and adherence are subjected to friction torque results in order to test if any improvement is achieved in bearing performance.

3.3.1. Stribeck Tests

Stribeck tests results are shown in Figure 13. At the beginning of the test, the four set of samples, Set 1, Set 2, Set 3 and baseline reach initial torque values between 6 and 6.5 N m. Then, during stabilization, Set 1 torque stabilizes at around 4 N m, Set 2 torque stabilizes at 3.2 N m and Set 3 torque stabilizes at 3 N m. However, baseline sample stabilizes at 1.3 Nm that is a very good result, much better than coated and polished bearings. Thus, as it can be checked, friction of coated bearings is never lower than friction consumed by uncoated bearings, so there is no improvement in tribological behavior of the bearings after coating at low load conditions.

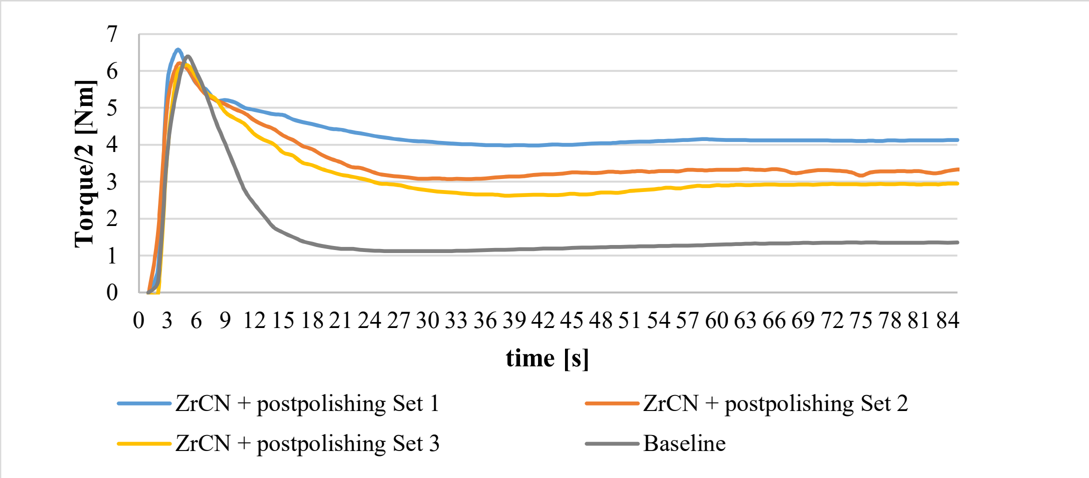

Figure 13. 594A / 592A ZrCN + postpolishing Stribeck friction test@8 kN.

3.3.2. TTR Tests

Figure 14 shows results for TTR tests. It can be observed that friction behavior is similar for all the bearing samples (Set 1, Set 2, Set 3, baseline) at low speed and loads. However, slight differences can be observed at high loads where Set 3 achieves torque values lower than baseline torque.

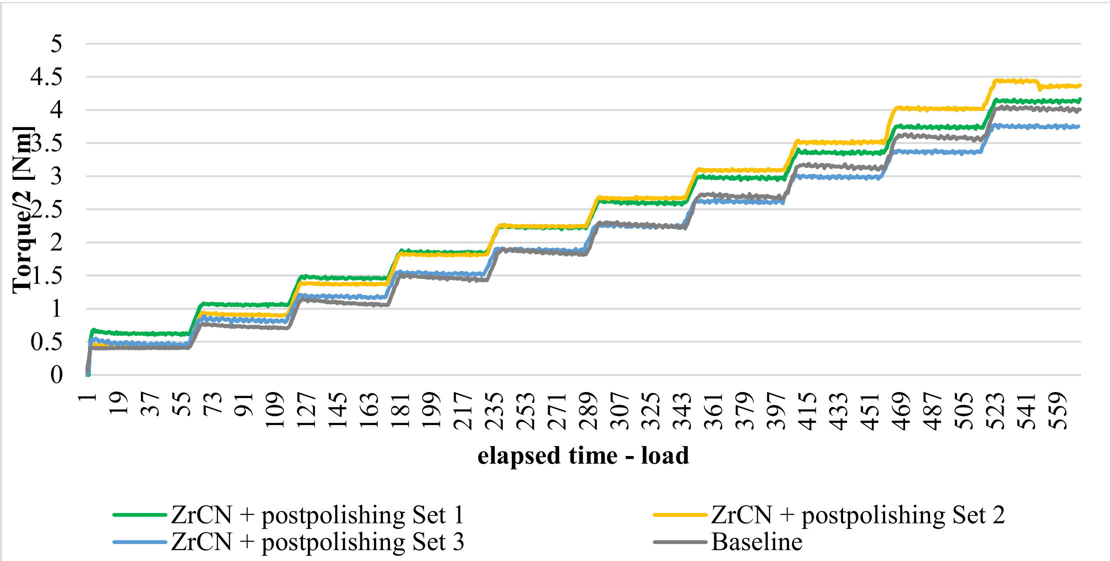

Figure 14. 594A/592A ZrCN + postpolishing TTR friction test@0–15 kN, 30 rpm.

Analyzing torque vs. load in Figure 15, it is shown that Set 3 exhibits a lower torque value than baseline for all the loads, which it is not achieved for Set 1 and Set 2. Dotted line shows average torque value for the three sets of coated bearings which shows that behavior is quite constant between the samples and no major torque improvement appears regarding baseline torque.

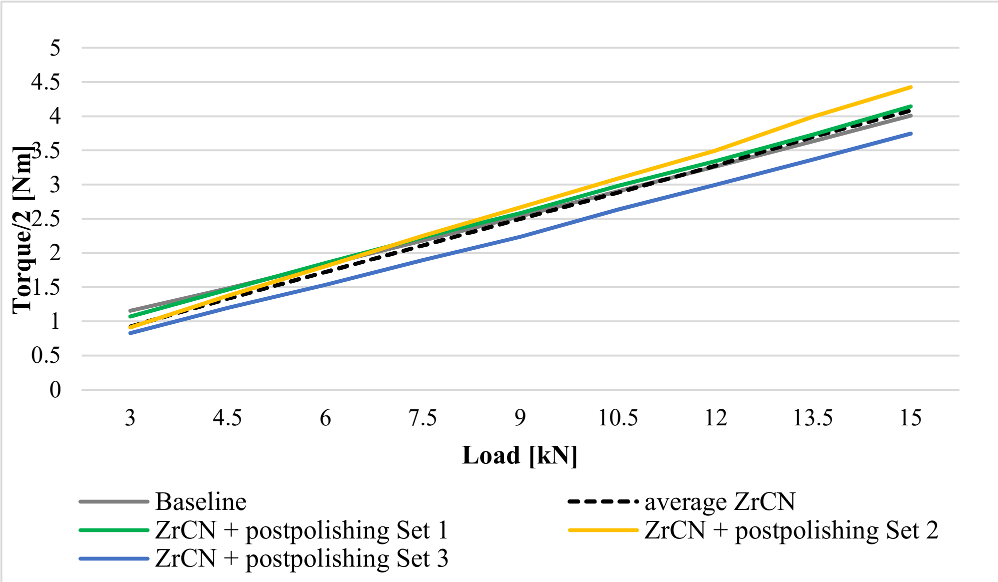

Figure 15. 594A/592A ZrCN + postpolishing TTR friction test vs. Baseline.

4. Conclusions

A strategy based on PVD coating of rolling bearings is proposed in order to improve friction during bearing performance. Different PVD coating designs have been tested varying composition and deposition time. Coatings with a longer deposition time obtain good adherence results although roughness allowed value of 0.15 is not achieved. Only samples coated with an interlayer of TiN instead of TiZr obtain acceptable roughness values at the expense of a bad adherence. A postpolishing process is proposed for the samples with good adherence in order to reduce roughness. Postpolishing method based on walnut shell additivated with a silica base abrasive 80% achieves proper roughness values of 0.082 on samples with a ZrN bilayer. These samples are subjected to friction torque test to evaluate their tribological behavior. Hardly any improvement is observed in the friction torque for the coated samples, neither at low load, nor at low speed.

Author Contributions: Conceptualization, G.M. and C.Z.; Methodology, G.M. and C.Z.; Software, G.M.; Validation, C.Z.; Formal Analysis, A.F., P.C. and A.L.; Investigation, A.L.; Resources, A.L., I.C. and D.E.; Writing–Original Draft Preparation, A.L.; Writing–Review & Editing, I.C.; Visualization, I.C. and D.E.; Supervision, I.C.; Project Administration, P.C. and A.F.; Funding Acquisition, P.C. and A.F.

Funding: This research was funded by Spanish Ministry of Industry, Economics and Competitivity (RTC-2016-5799-4).

Conflicts of Interest: The authors declare no conflict of interest. The founding sponsors had no role in the design of the study; in the collection, analyses, or interpretation of data; in the writing of the manuscript, and in the decision to publish the results.

References

1. Holmberg, K.; Andersson, P.; Nylund, N.-O.; Mäkelä, K.; Erdemir, A. Global energy consumption due to friction in trucks and buses. *Tribol. Int.* **2014**, *78*, 94–114.
2. Holmberg, K.; Matthews, A. Tribology of coatings. In *Coatings Tribology: Properties, Mechanisms, Techniques, and Applications in Surface Engineering*, 2nd ed.; Elsevier: Amsterdam, The Netherlands, 2009; p. 56.
3. Bhadeshia, H.K.D.H. Steels for bearings. *Prog. Mater. Sci.* **2012**, *57*, 268–435.
4. Dowson, D.; Higginson, G.R. Analysis of roller bearings. In *Elasto-Hydrodynamic Lubrication*, 1st ed.; Hopkins, D.W., Ed.; Elsevier: Amsterdam, The Netherlands, 1977.
5. Dowson, D. Elastohydrodynamic and micro-elastohydrodynamic lubrication. *Wear* **1995**, *190*, 125–138.

6. Dowson, D.; Higginson, G.R. Theory of roller bearing lubrication and deformation. *Proc. Inst. Mech. Eng.* **1963**, *177*, 67–69.
7. Harris, T.; Mindel, M. Rolling element bearing dynamics. *Wear* **1973**, *23*, 311–337.
8. Archard, J.F.; Crook, A.W. Apparatus and measurements of film thickness and film shape. In *Elasto-Hydrodynamic Lubrication*, SI ed.; Dowson, D., Higginson, G.R., Eds.; Pergamon Press: Oxford, UK, 1977; pp. 481–495.
9. Morales-Espejel, G.E.; Brizmer, V. Micropitting modelling in rolling–sliding contacts: Application to rolling bearings. *Tribol. Trans.* **2011**, *54*, 625–643.
10. Miller, G.R.; Keer, L.M.; Cheng, H.S. On the mechanics of fatigue crack growth due to contact loading. *Proc. Royal Soc. A* **1985**, *397*, 197–209.
11. Morales-Espejel, G.; Brizmer, V.; Piras, E. Roughness evolution in mixed lubrication condition due to mild wear. *Proc. Inst. Mech. Eng. Part J J. Eng. Tribol.* **2015**, *229*, 1330–1346.
12. Oh, H.; Azarian, M.H.; Morillo, C.; Pecht, M.; Rhem, E. Failure mechanisms of ball bearings under lightly loaded, non-accelerated usage conditions. *Tribol. Int.* **2015**, *81*, 291–299.
13. Clavería, I.; Elduque, D.; Lostalé, A.; Fernández, A.; Javierre, C.; Castell, P. Analysis of self-lubrication enhancement via PA66 strategies: Texturing and nano-reinforcement with ZrO_2 and graphene. *Tribol. Int.* **2019**, *131*, 332–342
14. Erdemir, A. Rolling-contact fatigue and wear resistance of hard coatings on bearing-steel substrates. *Surf. Coat. Technol.* **1992**, *54–55*, 482–489.
15. Kuhn, M.; Gold, P.W.; Loos, J. Wear and friction characteristics of PVD-coated roller bearings. *Surf. Coat. Technol.* **2004**, *174–175*, 469–476.
16. Igartua, A.; Laucirica, J.; Aranzabe, A.; Leyendecker, T.; Lemmer, O.; Erkens, G. Application of low temperature PVD coatings in rolling bearings: Tribological tests and experiences with spindle bearing systems. *Surf. Coat. Technol.* **1996**, *86–87*, 460–466.
17. Hochman, R.F. Rolling contact fatigue behavior of Cu and TiN coatings on bearing steel substrates. *J. Vacuum Sci. Technol. A* **1985**, *3*, 2348.
18. Rosado, L.; Jain, V.K.; Trivedi, H.K. The effect of diamond-like carbon coatings on the rolling fatigue and wear of M50 steel. *Wear* **1997**, *212*, 1–6.
19. Chang, T.-A.P.; Cheng, H.S.; Sproul, W.D. The influence of coating thickness on lubricated rolling contact fatigue life. *Surf. Coat. Technol.* **1990**, *43–44*, 699–708.
20. Komori, K.; Umehara, N. Effect of surface morphology of diamond-like carbon coating on friction, wear behavior and tribo-chemical reactions under engine oil lubricated condition. *Tribol. Int.* **2015**, *84*, 100–109.
21. Yeo, S.M.; Polycarpou, A.A. Fretting experiments of advanced polymeric coatings and the effect of transfer films on their tribological behavior. *Tribol. Int.* **2014**, *79*, 16–25.
22. Stewart, S.; Ahmed, R. Rolling contact fatigue of surface coatings—A review. *Wear* **2002**, *253*, 1132–1144.
23. Klaffke, D.; Santner, E.; Spaltmann, D.; Woydt, M. Influences on the tribological behaviour of slip-rolling DLC-coatings. *Wear* **2005**, *259*, 752–758.
24. Thom, R.; Moore, L.; Sproul, W.D.; Peter Chang, T. Rolling contact fatigue tests of reactively sputtered nitride coatings of Ti, Zr, Hf, Cr, Mo, Ti–Al, Ti–Zr and Ti–Al–V on 440 C stainless steel substrates. *Surf. Coat. Technol.* **1993**, *62*, 423–427.
25. Novak, R.; Polcar, T. Tribological analysis of thin films by pin-on-disc: evaluation of friction and wear measurement uncertainty. *Tribol. Int.* **2014**, *74*, 154–163.
26. Grill, A. Tribology of diamondlike carbon and related materials: an updated review. *Surf. Coat. Technol.* **1997**, *94–95*, 507–13.
27. Robertson, J. Diamond-like amorphous carbon. *Mater Sci. Eng. R Rep.* **2002**, *37*, 129–281.
28. Manier, C.-A.; Ziegele, H.; Barriga, J.; Goikoetxea, J.; Woydt, M. Zirconium-based coatings in highly stressed rolling contacts as alternativesolution to DLC and ta-C coatings. *Wear* **2010**, *269*, 770–781.
29. *ISO 683-17:2014 Heat Treated Steels, Alloy Steels and Free Cutting Steels—Part 17: Ball and Roller Bearing Steels*; ISO: Geneva, Switzerland, 2015.
30. Dinkel, M. Bearing steels and heat treatment. In Proceedings of ABMA Webinar Series, 17 September 2015. Available online: https://www.americanbearings.org/events/EventDetails.aspx?id=654049&hhSearchTerms=%22bearing+steels+and+heat+treatment%22 (accessed 17 September 2015).
31. IK4-Tekniker. Arc Evaporator and Method for Operating the Evaporator. International Patent WO2010072850, 7 January 2010.

32. *ISO 26423:2009 Fine Ceramics (Advanced Ceramics, Advanced Technical Ceramics)—Determination of Coating Thickness by Crater-Grinding Method*; ISO: Geneva, Switzerland, 2009.
33. *DIN EN ISO 4287:1998 Geometrial Product Specifications (GPS)—Surface Texture: Profile Method—Terms, Definitions and Surface Texture Parameters*; Deutsches Institut für Normung: Berlin, Germany, 1998.
34. *ISO 4287:1997 Geometrial Product Specifications (GPS)—Surface Texture: Profile Method—Terms, Definitions and Surface Texture Parameters*; ISO: Geneva, Switzerland, 1997.
35. *JIS B 0601:1994 Surface Roughness: Definitions and Designation*; JSA: Tokyo, Japan, 1994.
36. *ISO 4288:1996 Geometrial Product Specifications (GPS)—Surface Texture: Profile Method—Rules and Procedures for the Assessment of Surface Texture*; ISO: Geneva, Switzerland, 1996.
37. Verein Deutscher Ingenieure Normen. *VDI 3198 Coating (CVD, PVD) of Cold Forging Tool*; VDI-Verlag: Düsseldorf, Germany, 1991.
38. *ISO 1101:2017 Geometrical Product Specifications (GPS)—Geometrical Tolerancing—Tolerances of Form, Orientation, Location and Run-out*; ISO: Geneva, Switzerland, 2017.
39. Ebert, F-J. Fundamentals of Design and Technology of Rolling Element Bearings. *Chin. J. Aeronaut.* **2010**, *23*, 123–136.